Computer modeling of melting induced diapirism in the continental crust: plastic vs. creep rheology

O. P. Polyansky[a], A. V. Babichev[a], S. N. Korobeynikov[b], and V. V. Reverdatto[a]

[a]*Institute of Geology and Mineralogy, Siberian Branch, Russian Academy of Sciences, pr. Akad. Koptyuga 3, Novosibirsk, 630090 Russia, pol@uiggm.nsc.ru*

[b]*M. A. Lavrent'ev Institute of Hydrodynamics, Siberian Branch, Russian Academy of Sciences, pr. Akad. Lavrent'eva 15, Novosibirsk, 630090 Russia*

This paper is devoted to the modeling the granite-gneiss domes formation by means of diapiric upwelling. The granitic diapirism is widely developed in the Precambrian granite–greenstone belts, as well as in the metamorphic core complexes (Vanderhaeghe, 2009).

Geological settings. The diapiric structure can be illustrated by the Teya granite-gneiss dome located in the Trans-Angara portion of the Yenisei Ridge (Nozhkin et al., 1999). The dome structure (1500 km^2 in area) is the uppermost element of structurally and orographically uplifted sialic block in the central zone of the Yenisei ridge. The core part of the dome is made up of gneisses, granite gneisses, and gneiss-granites, as well as intrusive magmatic granite with average density of 2600 kg/m^3. Surrounding rocks are represented by the metamorphic sequences of the Proterozoic Teya and Sukhopit groups, which comprise aluminous garnet–staurolite–biotite crystalline schists (density of 2960 kg/m^3) and orthoamphibolites (2920 kg/m^3). The granitoids usually have concordant contacts with host rocks, but in some areas they exhibit cross-cutting relations. The Teya structure is distinguished as the large first-order uplift complicated by the second-order domes (Itui, Indol, Tyryda domes 6–10 km^2 in area). The latter are cut by ring and half-ring faults steeply dipping outward the dome.

Other examples of granite gneiss diapirs are Fangshan dome in the Northern Chinese Craton (He et al., 2009) and the Mt. Thor-Odin domes (Canadian Cordilleras) (Norlander et al., 2002). The parameters of the formation of the Fangshan dome structure are follows. SHRIMP U-Pb ages of zircons range from 128.5 to 132.4 Ma (Davis et al., 2001), while Ar/Ar data on biotite and hornblende (Ma. 1989) define close ages of cooling stage within 131.1–132 Ma. Based on the estimates obtained using Al_2SiO_5–K-feldspar geobarometer, the diapir was formed at pressure of 2 kbar, which corresponds to the intrusion depth of 6–7 km. The width of metamorphic zoning varies within the range of 300–2000 m at granodiorite core of the diapir of 8–10 km in size. The following zones are distinguished (from granodiorites outward): andalusite/sillimanite–K-feldspathic, garnet–staurolite, and andalusite–biotite zones, which correspond to the metamorphic temperatures from 450–500 to 650–700°C. Since no anatexis is observed within the aureole, the maximal temperature was no more than 675°C. The granodiorite core is rimmed by concentric zone of strike-slip deformations 200–600 m thick. Along periphery, the core is fringed by synclinal structure, which can be considered as signs of simultaneous deformation of the granitoids and host rocks during ascent of the diapir. The erosion of host metasediments above the upper part of the diapir was calculated by comparison with thickness of uneroded sedimentary rocks at the distance from domal structure and accounted for more than 4 km.

The parameters of diapir ascent of granitic magma obtained during geological analysis were applied for development of thermophysical and computer models described below.

Description of the model. A new approach is proposed in this work to outline the processes of partial melting and gravity instability in thickened crust with elevated thickness of granitic layer. The model was constructed to describe the melting and related upwelling of light material caused by underplating of basic magma at the base of continental crust. The aim of modeling consisted in determination of parameters of melting and diapirism in the lower crust.

Setting up the problem is shown in Fig. 1. A two-dimensional rectangular area of the Earth's crust 38 × 60 km in size (depth/width) is considered. The numerical modeling was performed using MSC.Marc software (Marc…, 2005), which involves all types of non-linearity of SM equations. The equations of quasi-static movement and thermal conductivity were solved for the upper region of modeling (in the upper 30 km), and only thermal conductivity equation was solved for the lower part (8 km).

The boundary conditions were taken as follows: upper boundary is the free surface with constant temperature T= 0°C; side boundaries are isolated from heat transfer and immobile with respect to mechanical movement in horizontal direction. The lower boundary is fixed in vertical direction and suggests free sliding along it. Initial conditions were taken as follows: the absence of initial displacements, lithostatic stress, temperature, corresponding to stationary geotherm at exponential distribution of radioactive heat sources throughout crust. It was suggested that the crustal base (middle part of the

model area 20 km wide) is intruded by basic melt with initial temperature of 1200°C, i.e., we consider the process of underplating. The constant temperature of (545°C) or constant mantle heat flow of 0.03 W/m^2 was assumed for the other part of the lower boundary.

It was suggested that the underplating area with intruded basic magma existed for 1–2 Ma, which caused the heating and partial melting of the overlying granitic crust. Underplating was estimated to have lasted for 1.6 Ma (Annen and Sparks, 2002), assuming repetitive magma replenishment and crustal growth by means of basic intrusions with total thickness of 8 km. For modeling, we used melting diagram of H2O-bearing granite. Results of two different approaches, elastoplastic and viscous rheology to the modeling the behavior of medium are given below.

Results with elastoplastic rheology. In this variant of model, the rheology of partially melted material and surrounding medium is governed by von Mises plasticity law. Versions of constant or temperature-dependent yield stress were considered. In the first case, the yield stress $<5_y$ varied from 1 MPa to 10 MPa. This range was selected on the basis of experimental data on viscoelastic behavior of medium (Bagdasarov and Dorfman, 1998), which indicate that the yield stress of partially melted granite containing about 40–50% melt accounts for less than 1 MPa

The results are shown as temperature field in a diapir body and set of isotherms beyond it. The first series of tests was conducted at constant temperature-independent yield limit σ_y = 1 MPa (Rosenberg, Handy, 2005). The results of modeling are shown in Fig. 2 as patterns of temperature field of intermediate states of upwelling melt. At the initial stage (duration of 2 Ma), the front of partial melting is spread over heat source. This provides only conductive heating and formation of partial melting area with immobile melt. The period of about 2 Ma involves the formation of the area with dome-like surface 6–7 km in height and width determined by given size of sheet basic intrusion (about 20 km) that caused heating. Then the melt area begins to rise (Fig. 2a–2c).

The second series of tests was carried out to study the effect of the temperature-dependent yield stress on dynamics of diapir upwelling. For these purposes, the upwelling height and diapir shape were determined by variations of the parameters σ_0, A_{pl}, and H_{pl} in the expression for temperature dependence of yield stress $\sigma_y = \sigma_0 + A_0\exp(-H_{pl}/RT)$. Figure 3 represents results of calculations according to the model of temperature-dependent plasticity, where the yield stress varies within 0.5–5 MPa for a range from melting temperature (650°C) to surface one. The comparison with previous model shows that two times decrease of the yield stress (from 1 to 0.5 MPa) leads to distinct pattern of upwelling. As in the previous case, the area of partial melt is formed as dome above basic intrusion; however, at a dome height of 5–6 km, its marginal parts begin to rise (Fig. 3a) such that the upwelling melt forms the cup-shaped body of complex geometry (Fig. 3b). This is followed by the formation of diapir leg, while material flows to periphery in horizontal direction at some constant deep level to form peripheral projections. With time, the latters reach the higher crustal levels (up to10–15 km) (Fig. 3c). Such diapirism could occur in the initially heated crust with high plasticity.

Results of creep rheology. The modeling results depend on many factors: geometrical (for instance, size of zone of crustal heating), temporal (duration of heating), and rheological (difference in densities, and values of coefficients in constitutive law). In this work, the main attention was focused on the rheology and heating duration. It was given that the time-limited heating lasted for 0.3 or 1.0 million years. In calculations, we varied the pre-exponential constant A_0, power-law exponent n, and activation energy Q of viscous flow $\eta = A^{-1/n}\,\varepsilon_{II}^{1-n/2n}\exp(Q/nRT)$. The change in pre-exponential constants causes a change in the upwelling rate, but shows no effect on the diapir shape. The rheological constants were taken in accordance with (Ranally, 1995): $A_0 = 0.5\ 10^{-17}$ Pa^{-n} s^{-1}, n = 2.3, Q = 154 kJ/mol. In addition, a finite duration of heating (1 Ma) was given. Results are shown in Fig. 4 for the time moments of 0.6, 1, and 1.24 Ma at heating (Figs. 4a and 4b) and cooling (Fig. 4c) stages. There are some differences as compared to previous variants. First, two projections (plumes) are formed in the vicinity of basic intrusion, which then are merged in a single plume (Figs. 4a, b). Diapir is spread horizontally within lower crust and forms batholite-shaped body about 40 km wide at initial width of the heating zone of 20 km. Second, unlike the previous cases, the maximal depth of upwelling is limited and does not exceed 20 km. At a distance from diapir, this depth approximately corresponds to stationary isotherm of 400°C. These calculations show that the upwelling height is limited by some depth level, above which deformations becomes insignificant due to low temperature of the medium.

In the last series of experiments we employed a viscous-elastic-plastic rheology with a temperature-dependent viscosity and von Mises plasticity. In this experiment we observe that the diapir head intrudes through the whole of crust (Fig. 5).

Geological implications and conclusions. The following conclusions can be drawn from model calculations:

1. The rheology of crust plays a significant role in modeling diapirism. The modeling rates of diapir upwelling in the elastic-plastic crust are orders of magnitude higher (meters to tens meters per year) than those obtained by modeling in the framework of creep rheology (0.8 cm/yr).

2. Estimated depth of diapir roof (20 km) (Fig. 4) corresponds well to the maximal upwelling level (15 km) obtained in numerical modeling of (Bittner and Schmelling, 1995) for viscous rheology of “softer” crust. However, our calculations for the elastic-viscous-plastic rheology demonstrated the possible upwelling at shallower levels, as it was found for many natural geological settings (He et al., 2009).

3. Modeling results revealed the limited depth of upwelling of partially crystallized melt (corresponding to isotherm of 400°C) in the case, when temperature

dependence of creep properties is taken into account (model of Fig. 4). The same temperature barrier is indicated as limiting level of magma ascent in (Vanderhaeghe, 2009).

4. Upwelling with formation of pair diapirs from a single melting area is provided in both variants (with elastic-plastic and viscous-plastic rheology, Figs. 3 and 4). Natural migmatite domes typically correspond to the structures of second order, which are interpreted as phases of repetitive magma intrusion. Pair structures of the second order can be exemplified by the Itui and Tyryda domes in the Teya granite-gneiss diapir, which are located at 25 km distance from each other. Our model results make it possible to explain the formation of two or several diapiric cores from a single magmatic source.

1. A. D. Nozhkin, O. M. Turkina, E. V. Bibikova, et al., "Riphean Granite-Gneiss Domes of the Yenisei Range: Geological Structure and U-Pb Isotope Age," Russ. Geol. & Geophys. 40 (9), 1305-1313 (1999).
2. B. He, Y.-G. Xu, S. Paterson, Magmatic diapirism of the Fangshan pluton, southwest of Beijing, China, Journal of Structural Geology 31, 615–626 (2009).
3. D. Bittner and H. Schmeling, "Numerical Modeling of Melting Processes and Induced Diapirism in the Lower Crust," Geophys. J. Int. 123, 59-70 (1995).
4. O. Vanderhaeghe, Migmatites, Granites and Orogeny: Flow Modes of Partially-Molten Rocks and Magmas Associated with Melt/Solid Segregation in Orogenic Belts, Tectonophysics 477, 119-134 (2009).
5. C. Rosenberg and M. R. Handy, "Experimental Deformation of Partially Melted Granite Revisited: Implications for the Continental Crust," J. Metamorph. Geol. **23**, 19-28 (2005).
6. Marc User's Manual. Vol. A: Theory and Users Information (MSC Software Corp., Santa-Ana, 2005).
7. G. Ranalli, Rheology of the Earth (Chapman & Hall, London, 1995).

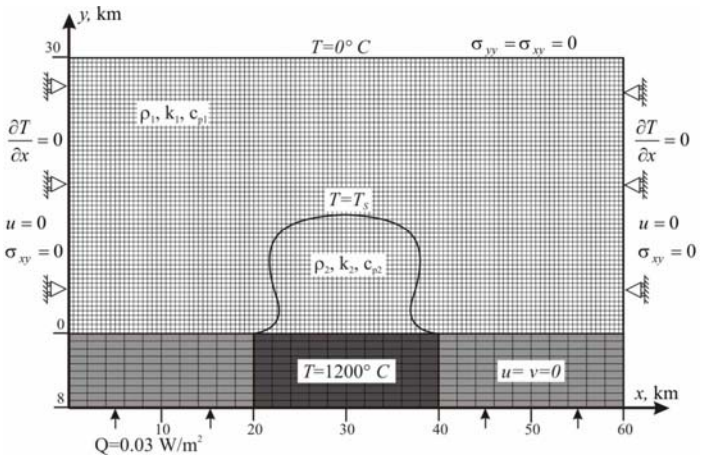

Fig. 1. Setting up the problem of melting and diapirism in the lower crust. Shown are the modeling areas, parameters, boundary and initial conditions, initial numerical grid of finite elements. Basic magma (dark gray) with initial temperature of 1200 ºC intruded immobile medium of the lower crust (gray). Thin solid line denotes the melting boundary, which separates the partially crystallized melt and host rocks with different properties.

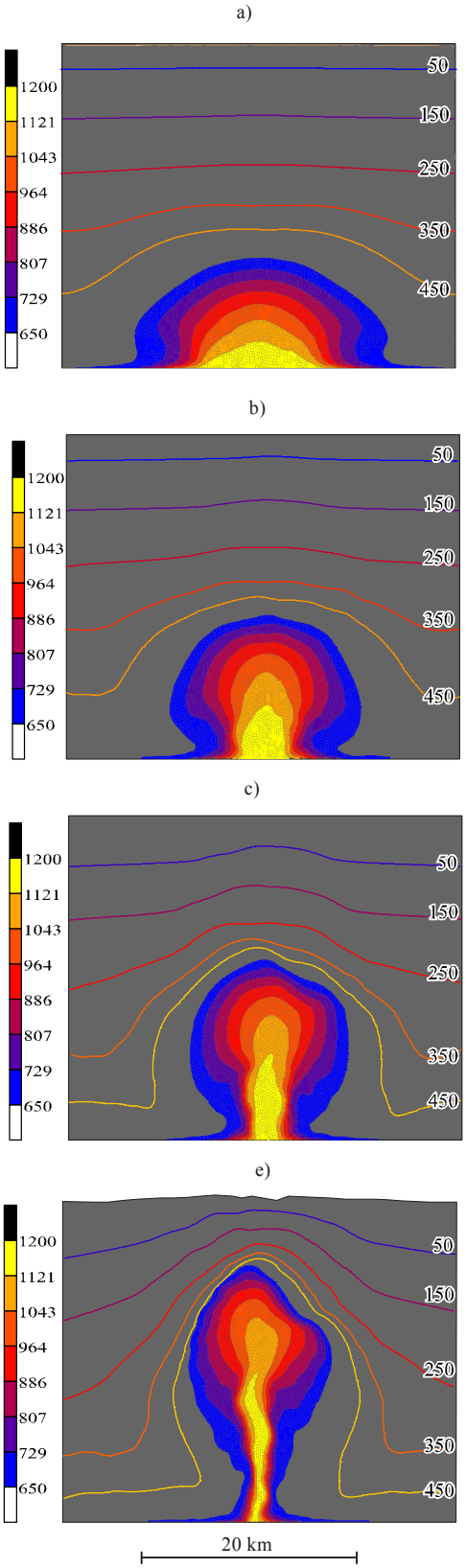

Fig. 2. Evolution of diapir upwelling assuming constant yield stress of crustal material. Shown is the middle part of model area (sizes are in km), with pattern of temperature field in the diapir body (in color scale) and beyond it (in isothrms, in °C). The snapshots are not at equidistant time intervals: from onset of upwelling (a) to moment of time of 2.159 Ma (c). Scale in range of 650-1200°C is shown on the left. Gray field shows the area with temperature, below solidus (650°C).

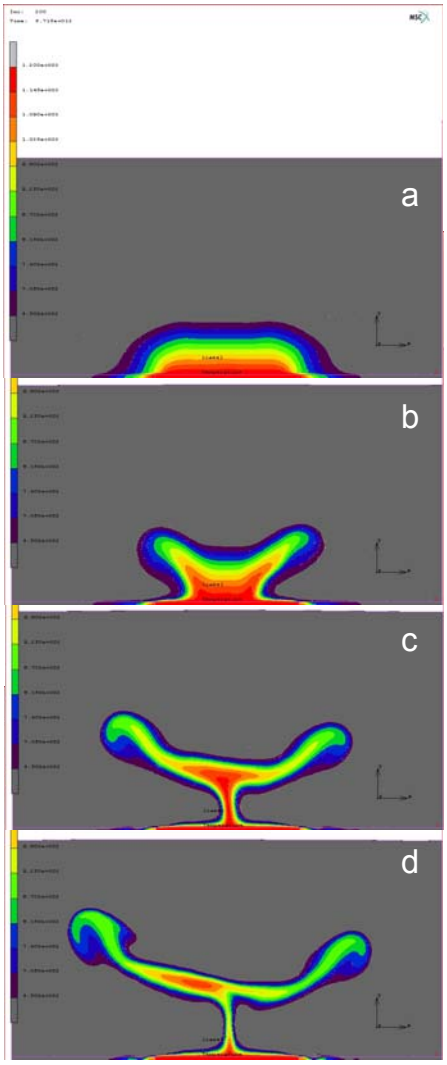

Fig. 3. Results of modeling of the diapir upwelling under temperature dependent yield stress. Temperature field in the diapir beginning from onset of upwelling (a) and up to 2.132 Ma (c). .Model area is shown as in fig. 2. Temperature scale (in °C) is shown in the left.

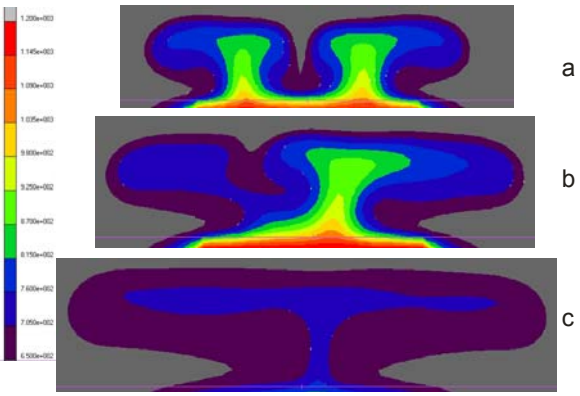

Fig. 4. Evolution of melting front and granite diapir geometry using the visco-elastic rheology at 0.67 (a), 1 (b) and 1.44 (c) Myr. Zoomed central part of lower crust (30 km wide, in depth from 20 to 30 km). Stages (a), (b) – heating, stage (c) – cooling.

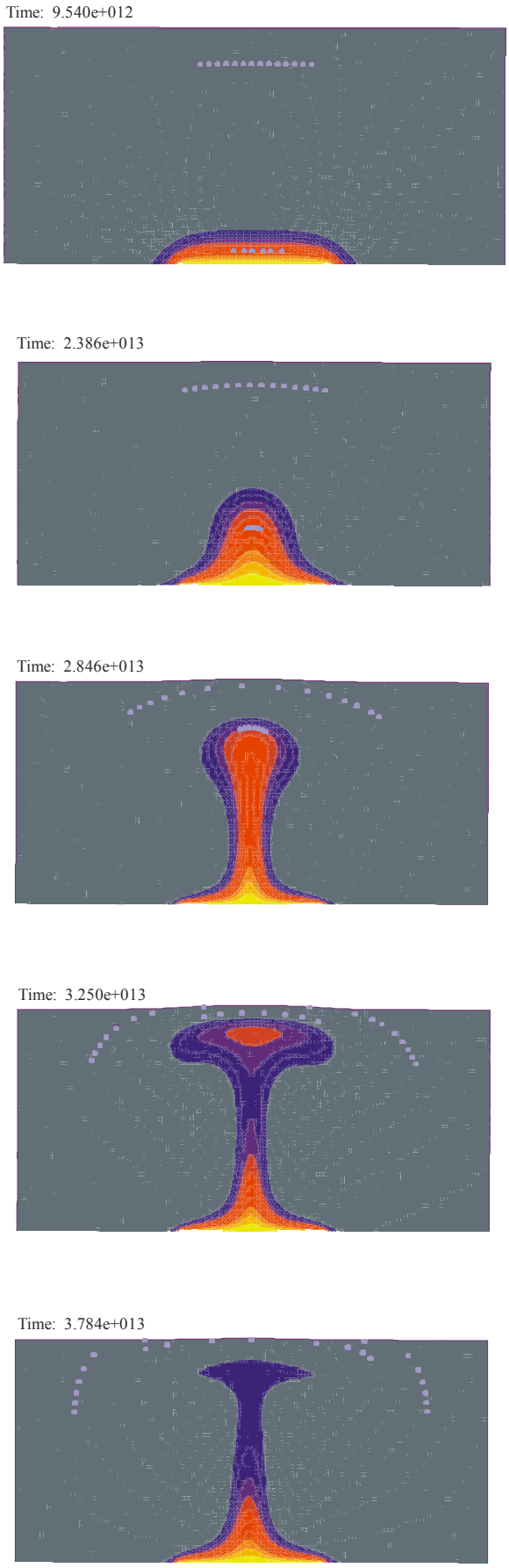

Fig. 5. Temperature and diapir geometry evolution using a visco-elastic-plastic rheology . Model area is shown as in fig. 1.). The snapshots are shown at 0.3, 0.75, 0.9, 1 and 1.2 Myr. Temperature scale – as in Fig. 2.